

Control of PD-L1 Expression by Oncogenic Activation of the AKT–mTOR Pathway in Non-Small Cell Lung Cancer

Kristin J. Lastwika^{1,2}, Willie Wilson III³, Qing Kay Li⁴, Jeffrey Norris¹, Haiying Xu⁵, Sharon R. Ghazarian⁶, Hiroshi Kitagawa¹, Shigeru Kawabata¹, Janis M. Taube⁵, Sheng Yao⁷, Linda N. Liu⁷, Joell J. Gills¹, and Phillip A. Dennis¹

Abstract

Alterations in EGFR, KRAS, and ALK are oncogenic drivers in lung cancer, but how oncogenic signaling influences immunity in the tumor microenvironment is just beginning to be understood. Immunosuppression likely contributes to lung cancer, because drugs that inhibit immune checkpoints like PD-1 and PD-L1 have clinical benefit. Here, we show that activation of the AKT–mTOR pathway tightly regulates PD-L1 expression *in vitro* and *in vivo*. Both oncogenic and IFN γ -mediated induction of PD-L1 was dependent on mTOR. In human lung adenocarcinomas and

squamous cell carcinomas, membranous expression of PD-L1 was significantly associated with mTOR activation. These data suggest that oncogenic activation of the AKT–mTOR pathway promotes immune escape by driving expression of PD-L1, which was confirmed in syngeneic and genetically engineered mouse models of lung cancer where an mTOR inhibitor combined with a PD-1 antibody decreased tumor growth, increased tumor-infiltrating T cells, and decreased regulatory T cells. *Cancer Res*; 76(2): 227–38. ©2015 AACR.

Introduction

Despite the development of targeted therapies, lung cancer remains the leading cause of cancer-related death worldwide (1). Most of the oncogenic drivers in non-small cell lung cancer (NSCLC), such as EGFR or KRAS, activate the PI3K–AKT–mTOR pathway, which increases cell proliferation, metabolism, and survival. Activation of this pathway is a critical event during lung tumorigenesis. Previously, we showed that genetic deletion of AKT1 or inhibitors of mTOR such as rapamycin or metformin prevent KRAS-driven lung tumorigenesis (2–4). We also demonstrated a relationship between AKT/mTOR signaling and immune suppression, because inhibition of tumorigenesis by rapamycin was associated with reduced influx of lung associated FoxP3⁺ regulatory T cells (Tregs) into the tumors (5). This was confirmed by creating mice that harbored mutant KRAS but lacked FoxP3

cells. Mice that lacked FoxP3 cells developed fewer lung tumors than mice with mutant KRAS alone.

Although multiple mechanisms can contribute to immune suppression in the tumor microenvironment, programmed death ligand 1 (PD-L1 and B7-H1), an inhibitory member of the B7 family, plays a central role in many cancer types (6). This cell surface protein is normally found on immune cells and in immune privileged tissues, but its expression is upregulated in many epithelial tumors, including lung cancer (7). PD-L1 binds to either PD-1 or CD80 receptors on activated immune cells to inhibit their activation and effector responses (8). The interaction of PD-L1 and PD-1 induces differentiation of naïve CD4⁺ T cells into Tregs and maintains Treg-suppressive functions. PD-L1 can also act as a receptor by sending reverse signals to limit tumor cell apoptosis. The importance of PD-L1 and PD-1 in lung cancer is reflected by the antitumor activity observed using PD-1- or PD-L1-blocking antibodies as single agents in heavily pretreated NSCLC patients (9, 10). Clinical responses were sometimes sustained over many months, suggesting recovered ability of immune effectors to control tumor growth (11). This clinical benefit supports efforts to study the mechanisms that regulate tumor PD-L1 expression and therapeutic interventions to decrease PD-L1 levels.

Tumors can express PD-L1 either constitutively or through induction by inflammatory cytokines, especially members of the interferon family. Cytokine-driven PD-L1 expression is indicative of an ongoing immune response in the tumor microenvironment, whereas intrinsic PD-L1 expression does not depend on the presence of tumor-infiltrating lymphocytes.

Multiple mechanisms can contribute to intrinsic tumor PD-L1 expression. Expressions of PD-L1 and PD-L2 (another ligand for PD-1) are increased in Hodgkin's disease and mediastinal large B-cell lymphoma through chromosomal amplification (12). T-cell

¹Department of Oncology, Johns Hopkins University, Baltimore, Maryland. ²The George Washington University, Institute for Biomedical Sciences, Washington, DC. ³Cancer Biology and Genetics Branch, Center for Cancer Research, National Institutes of Health, Bethesda, Maryland. ⁴Department of Pathology, Johns Hopkins University, Baltimore, Maryland. ⁵Department of Dermatology, Johns Hopkins University, Baltimore, Maryland. ⁶Biostatistics, Epidemiology and Data Management Core, Johns Hopkins University, Baltimore, Maryland. ⁷Amplimmune, Inc., Gaithersburg, Maryland.

Note: Supplementary data for this article are available at Cancer Research Online (<http://cancerres.aacrjournals.org/>).

Corresponding Author: Phillip A. Dennis, Johns Hopkins University School of Medicine, 4940 Eastern Avenue, 301 Building/Suite 4500 Baltimore, MD 21224. Phone: 410-550-9250; Fax: 410-550-5445; E-mail: pdennis@jhmi.edu

doi: 10.1158/0008-5472.CAN-14-3362

©2015 American Association for Cancer Research.

lymphomas carrying NPM-ALK fusions induce PD-L1 expression through STAT3 activation (13). PTEN loss or PIK3CA mutations in glioma, breast, and prostate cancers have been shown to activate the AKT-mTOR pathway and subsequently increase PD-L1 expression (14, 15). A correlation between activating mutations in EGFR and increased immunosuppression markers, including PD-L1 and PD-1, was established (16). Recently, a mouse model of lung squamous carcinoma demonstrated high PD-L1 expression in tumor-promoting cells with loss of LKB1 and PTEN (17). In NSCLC patients, the relationship of oncogenic drivers with PD-L1 expression is still unclear with one study associating PD-L1 expression with mutant EGFR but not KRAS or ALK (18), and another demonstrating no clear difference in PD-L1 staining between samples with mutations in EGFR, KRAS, or ALK (19). Because the AKT-mTOR pathway serves as a convergence point for activation of many of the oncogenes involved in NSCLC, we hypothesized that this pathway was likely responsible for the control of PD-L1 expression. We used NSCLC cell lines, mouse models, and primary human lung cancers to show that PD-L1 protein expression is dependent on active AKT-mTOR signaling, regardless of specific oncogenic or cytokine stimuli. These data identify a common mechanism of PD-L1 regulation in lung cancer, and provided rationale for clinical trials of oncogenic pathway inhibitors combined with inhibitors of immune checkpoints.

Materials and Methods

Cell culture

CL30, IO33, CL13, and CL25 cell lines were derived from 4-(Methylnitrosamino)-1-(3-pyridyl)-1-butanone (NNK)-induced lung adenocarcinomas developed in A/J mice, and were a generous gift from Dr. Steven Belinsky (Lovelace Respiratory Research Institute, Albuquerque, NM) in 1999 (20). Immortalized Beas2B and isogenic Beas2B transformed with NNK have been described previously (21). HCT-116 parent, PTEN^{-/-}, PIK3CA mutant or KrasD13^{-/-} isogenic cells were obtained from the JHU Genetic Resources Core Facility. Human lung cancer cell lines were early passages (<20) of the original cell lines from the National Cancer Institute obtained in the years spanning 2000 to 2012. H1975 and H157 cell lines had higher passages (>20) and were authenticated by JHU Genetic Resources Core Facility. H1299 was authenticated by DDC Medical in 2012. Immortalized Beas2B and isogenic Beas2B transformed with NNK were a gift in 1996. HCT-116 parent, PTEN^{-/-}, PIK3CA mutant or KrasD13^{-/-} isogenic cells were obtained from the JHU Genetic Resources Core Facility in 2012. All cell lines were passaged for fewer than 6 months after resuscitation.

Transfections

CL13 cells were transfected with DharmaFECT (Thermo Scientific) and a pool of 4 mouse PTEN siRNA or scrambled siRNA (L-040700-00-0005; Thermo Scientific). The pLKO.1 plasmids containing shRNA targeted to human RAPTOR or RICTOR have been described previously (22).

Mouse models

All animal studies were conducted using a protocol approved by the Animal Care and Use Committee at the National Cancer Institute. The genetically engineered KRAS^{LA2} and CC10⁺ EGFR^{L585R/T790M} mice, as well as, the NNK-induced A/J mouse lung tumor model have been described previously (3, 23, 24).

In vivo treatments

For the transgenic KRAS^{LA2} mouse model treatment began at weaning and lasted 4 weeks. One hundred and fifty micrograms of anti-PD-1 blocking antibody (Amplimmune) was given on the first treatment day in combination with rapamycin. The control vehicle was given on treatment day 1 in combination with 150 µg IgG (Rockland). A previously optimized rapamycin dosing schedule was used to obtain trough levels that are readily tolerated in humans (25). The control and anti-PD-1 antibody were given by i.p. injection once a week for 3 wks and tumors were harvested 1 hour after the last injection. Mice were weighed QOD to monitor for toxicity. Tumor burden was calculated as the sum of individual lung tumor volumes per mouse.

Immunoblotting

Cell lysates were prepared in 2xLSB. Antibodies were from Cell Signaling Technology unless otherwise noted and included anti-PD-L1 antibody (AbCam; ab58810), anti-phospho-AKT^{S473} (9271), anti-AKT (9272), anti-phospho-S6 (4858), anti-S6 (2317), anti-phospho-ERK^{T202/Y204} (4370) anti-ERK (4695), anti-phospho-EGFR^{Y1068} (3777), anti-EGFR (4267) anti-mutant EGFR^{L585R} (3197), anti-phospho-AMPK^{T172} (2535), anti-AMPK (2532), anti-phospho-ACC^{S79} (3661), anti-ACC (3662), anti-RAPTOR (2214), anti-RICTOR (2114), anti-phospho-4E-BP1^{S65} (9451), anti-4E-BP1 (9644), anti-phospho-JAK2^{Y1007/1008} (3771), anti-JAK2 (3230), anti-phospho-STAT3^{Y705} (9145), anti-STAT3 (8768), anti-p53 (2524), anti-p21 (2947), and anti-αtubulin (Sigma-Aldrich; T5168).

Quantitative RT-PCR for PD-L1

RNA was isolated from CL13 cells using the Qiagen RNeasy Mini Kit (Qiagen). cDNA was made using the SuperScript II RT Reaction Kit (Invitrogen) from 2 µg of isolated RNA. PD-L1 (Mm00452054_m1) specific and control 18S (Mm03928990_g1) primers were purchased from Applied Biosystems. Samples were analyzed on a StepOnePlus RT-PCR System Instrument using TaqMan Universal PCR Master Mix, No AmpErase UNG (Applied Biosystems) according to the manufacturer's instructions.

Flow cytometry

A total of 1×10^6 human and mouse lung cancer cells were harvested and stained for 30 minutes at 4°C with primary antibody to PE-anti-mouse-PD-L1 (BioLegend; #10F.9G2), PE-anti-mouse-B7-H4 (eBioscience; Clone 188), PE-anti-human-PD-L1 (eBioscience; Clone M1H1), APC-anti-human-B7-H4 (BD Pharmingen; Clone M1H43) or isotype-matched controls. Samples were run on a FACS Caliber (BD Biosciences) and analyzed using FlowJo software (TreeStar).

Immunohistochemistry

Formalin-fixed lung tissues were incubated in PD-L1 (CST# 13684), pS6^{S235/235} (CST#4858), FoxP3 (eBio #14-5773-82), CD3 (A0452 Dako), Ki67 (Ab16667 AbCam), Cleaved caspase-3 (CST#9664), pHP-1 gamma (ab45270 AbCam), and detection was completed using the VECTASTAIN Elite ABC Kit (Vector Laboratories) per the manufacturer's instructions. Tissues were also incubated in the presence of an isotype-matched control antibody (sc-2027; Santa Cruz Biotechnology). All stains were quantified in 10 tumor-containing $\times 40$ magnification fields. For

murine PD-L1, the percentage of positive tumor cell surface staining was scored as (<5%), 1+ (≥5–20%), 2+ (≥20%–50%) or 3+ (≥50%). pS6 staining was quantified by assigning a score of absent (0), minimal (1), moderate (2), or strong (3) to each tumor. The staining index was calculated for each tumor by multiplying the staining intensity by its distribution. FoxP3, CD3, Ki67, Cl. Caspase-3 and pHP-1 γ stains were quantified by counting the number of positive cells. The investigator was blinded to sample identities during scoring.

TMA slides were stained with the 5H1 antibody for PD-L1 expression and a mouse IgG isotype antibody using a previously described protocol by a board certified pathologist (Q.K. Li; ref. 26). Approximately 10% of randomly chosen cores were scored to confirm PD-L1 by a second board certified pathologist (J.M. Taube). Both TMAs were also analyzed for pS6^{S235/236} (CST#4858) expression. Tumor with >10% phospho-S6 expression were considered positive.

Statistical analysis

Data in bar graphs are presented as mean \pm SE. χ^2 analyses tested for differences between the distributions of clinical variables across histologic samples. The Fisher exact test examined potential statistical associations of the association between PD-L1 and phospho-S6 expression in both TMAs. Quantification of

immunoblotting was analyzed by unpaired the Student *t* test. Tumor volume and tumor-infiltrating lymphocytes were analyzed by two-way ANOVA followed by Tukey's *post hoc* test. Statistical significance was reached with a *P* value less than or equal to 0.05.

Results

Expression of PD-L1 in mutant EGFR and mutant KRAS murine lung tumors

PD-L1 expression was examined in mouse models of lung cancer driven by activating mutations in KRAS or EGFR that are used to model lung cancer in smokers and never smokers, respectively. In the KRAS^{LA2} mouse model, lung adenocarcinomas develop after spontaneous recombination events induce oncogenic KRAS^{G12D} expression. Immunoblotting of lung lysates from KRAS^{LA2} mice demonstrated increased activation of AKT/mTOR and PD-L1 expression compared with age-matched, wild-type littermates (Fig. 1A). EGFR^{L858R/T790M} mice have doxycycline-inducible expression of human mutant EGFR. Lung lysates harvested from mice exposed to doxycycline for 3 weeks show increased expression of EGFR, active AKT/mTOR signaling and PD-L1 (Fig. 1A, middle). The tobacco-specific carcinogen NNK induces KRAS mutations and causes primarily lung adenomas in susceptible mouse strains. We previously showed that activation of the AKT–mTOR pathway is critical for NNK-induced lung

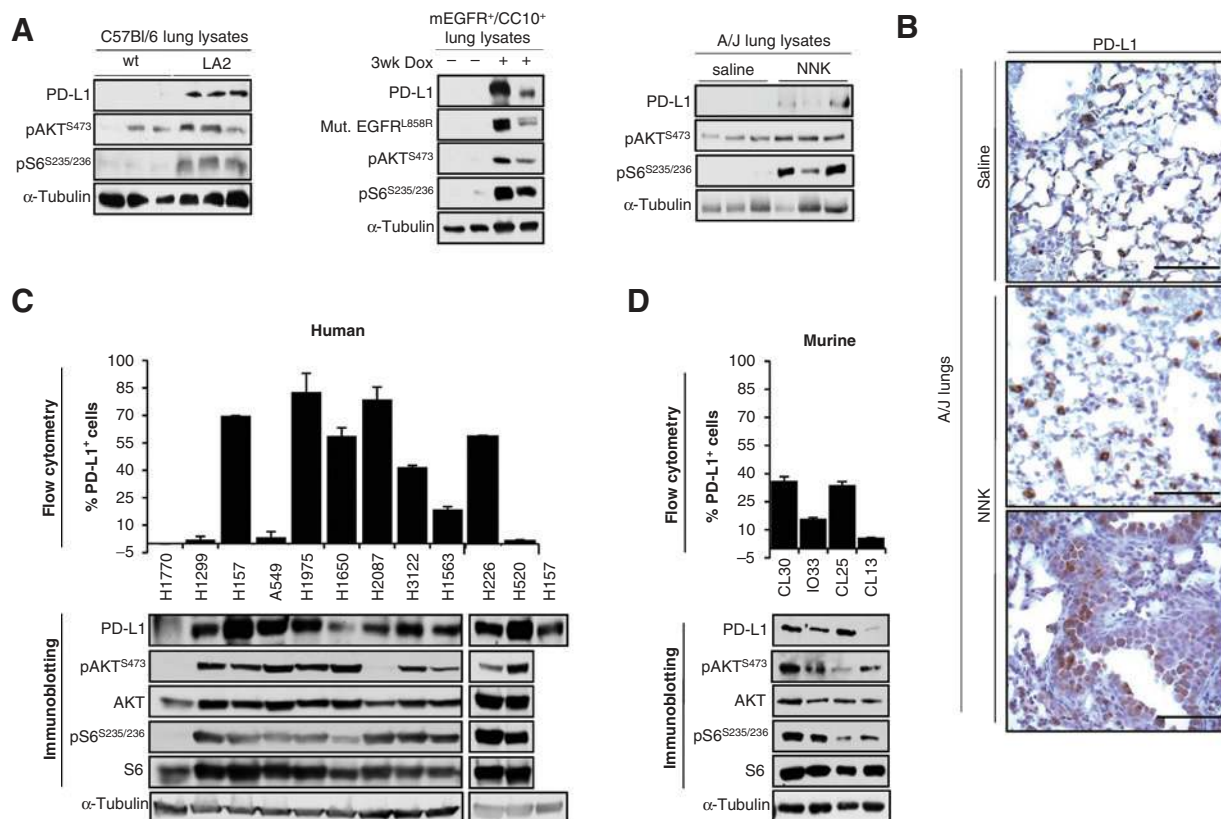


Figure 1. Expression of PD-L1 and oncogenic activation of the Akt–mTOR pathway. A, lung lysates were harvested from C57Bl/6 KRAS LA2 or wt littermates (left), from FVB mEGFR⁺/CC10⁺ littermates treated with or without doxycycline (middle), or from A/J mice exposed to i.p. saline or the tobacco carcinogen NNK (right), and processed for immunoblotting. Each lane represents one mouse. B, A/J mice treated as in A showing PD-L1 expression in lung lesions but not in normal lung epithelium. Scale bar, 10 μ m. C and D, human NSCLC cell lines (C) and NNK-derived murine lung adenocarcinoma cell lines (D) have activation of AKT–mTOR, as well as expression of PD-L1 as shown by flow cytometry and immunoblotting.

tumorigenesis (27). In lung lysates from 1-year-old mice previously treated with NNK, PD-L1 expression was observed in NNK- but not saline-exposed lungs. Lungs from NNK-treated mice also had higher activation of AKT and mTOR (Fig. 1A, right). IHC staining of lung tissues from mice demonstrates PD-L1 expression in resident immune cells but not in normal lung epithelium (Fig. 1B, top and middle). In contrast, PD-L1 was detected in early lung lesions after a single NNK exposure. Collectively, these data demonstrate that PD-L1 is expressed in mouse models of NSCLC driven by mutations in KRAS or EGFR.

Expression of PD-L1 and AKT/mTOR activation in NSCLC cell lines

NSCLC cell lines were examined for total PD-L1 expression by immunoblotting, and membranous PD-L1 expression by flow cytometry. The panel of human cell lines was chosen to include a variety of oncogenic drivers, in an effort to reflect the mutational spectrum seen in patients. AKT/mTOR activation was detected in adenocarcinoma and squamous cell carcinoma cell lines with mutations in NRAS (H1299), KRAS (H157/A549), EGFR (H1975/H1650), BRAF (H2087), PIK3CA (H1650), EML4-ALK (H3122), RET (H1563), autocrine production of FGF2 (H226), or FGFR1 amplification (H520; Fig. 1C). These cell lines expressed

PD-L1 by immunoblotting and flow cytometry. The H1770 (NOTCH1) cell line did not have active AKT/mTOR signaling or express PD-L1. Murine cell lines established from NNK-induced lung adenocarcinomas also had AKT/mTOR activation and PD-L1 expression (Fig. 1D). Expression of PD-L1 in these cell lines appeared selective, because expression of another immunosuppressive ligand, B7-H4, was only observed in $\leq 10\%$ of cells for all but one cell line tested (H520; Supplementary Fig. S1A). These studies show that activation of AKT and mTOR is associated with PD-L1 expression in NSCLC lines that harbor a wide spectrum of driver mutations.

Inhibition of PI3K, AKT, or mTOR decreases PD-L1 expression in NSCLC cell lines

To test whether PD-L1 expression was dependent on active PI3K-AKT-mTOR signaling, murine and human NSCLC cell lines with mutations in KRAS or EGFR and high PD-L1 expression were treated with pharmacologic inhibitors of components in the pathway. Inhibitors of PI3K (LY294002), AKT (TCN-P), or mTOR (rapamycin) decreased PD-L1 expression in a time-dependent manner (Fig. 2A-C). Although some cell line specificity was observed, inhibition of PI3K, AKT, and mTOR activity appeared to coincide with or precede decreased PD-L1 expression. After

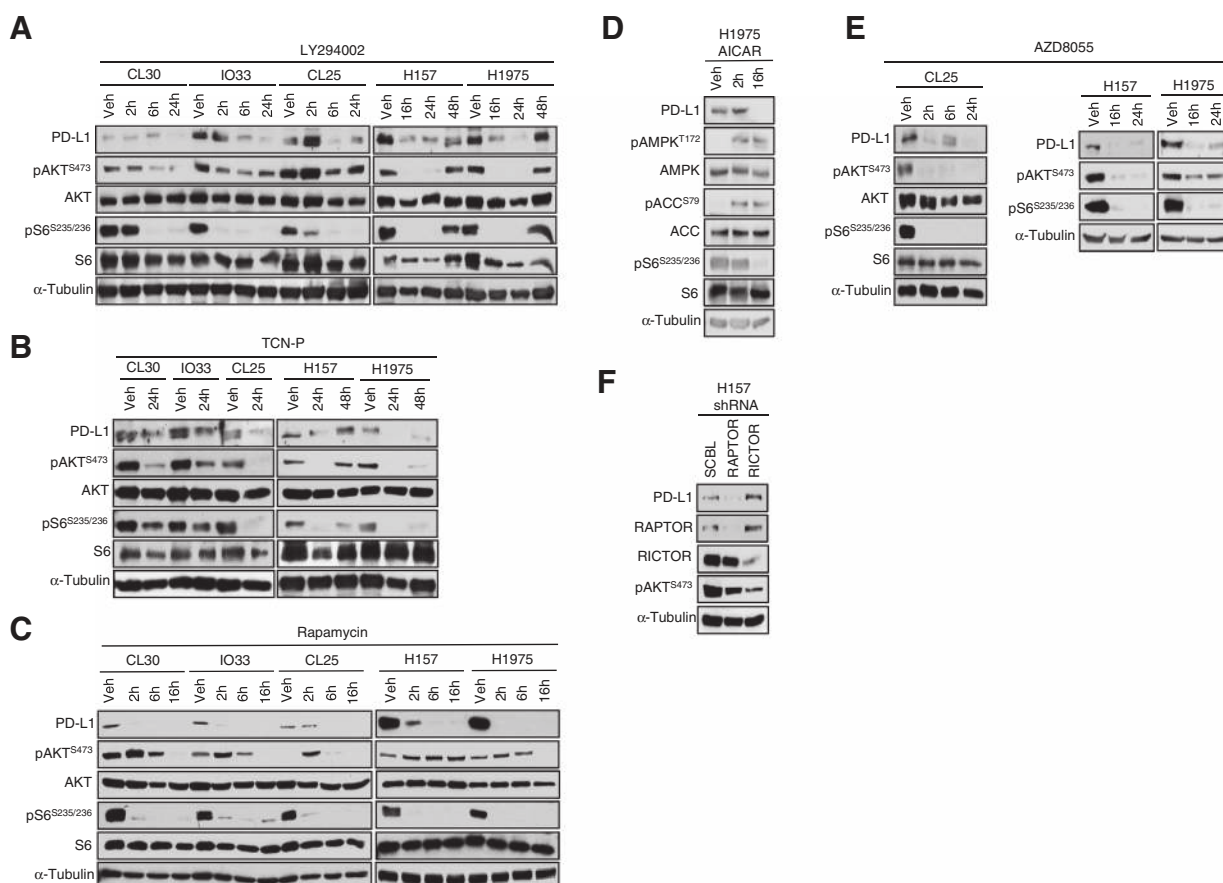


Figure 2.

Inhibition of the PI3K-AKT-mTOR pathway decreases PD-L1 expression. A-C, NSCLC cell lines were treated with 10 $\mu\text{mol/L}$ of a PI3K inhibitor (LY294002; A) 1 $\mu\text{mol/L}$ of an AKT inhibitor (TCN-P; B), or 100 nmol/L of an mTOR inhibitor (rapamycin; C). D, cells were treated with 2 mmol/L AICAR or vehicle. E, cell lines were treated with 100 nmol/L of a dual mTORC1/2 inhibitor (AZD8055). F, stable shRNA knockdown of RAPTOR (mTORC1) but not RICTOR (mTORC2) decreases PD-L1 in H157 cells (A-F).

48 hours of PI3K or AKT inhibition, recovery of pathway activation and expression of PD-L1 occurred with similar kinetics in cell lines. In contrast, recovery of mTOR activity or PD-L1 expression was not observed with rapamycin at the time points examined, possibly due to its long half-life. To investigate whether PI3K and AKT inhibition were required for mTOR inhibition and decreased expression of PD-L1, we used AICAR, an activator of AMPK that can inhibit mTOR independently of PI3K and AKT. AICAR activated AMPK, increased phosphorylation of the AMPK substrate ACC, inhibited mTORC1 activation, and decreased PD-L1 expression at 16 hours (Fig. 2D). Taken together, these results demonstrate that inhibition of PI3K, Akt, or mTOR (through allosteric inhibition with rapamycin or AMPK activation), decreases PD-L1 expression.

To confirm the results obtained with rapamycin and AICAR, we also tested a dual mTORC1/2 inhibitor, AZD8055. AZD8055 decreased PD-L1 expression coincident with decreased activation of AKT and mTOR (Fig. 2E). Because inhibition of PD-L1 by rapamycin correlated more closely with inhibition of pS6 but not pAKT at early time points, this suggested that mTORC1 exerts more control over PD-L1 expression than mTORC2. To discern whether PD-L1 expression is dependent on mTORC1 or mTORC2, shRNA-mediated knockdown of a key component in mTORC1 (RAPTOR) or mTORC2 (RICTOR) was performed in H157 cells. Knockdown of RAPTOR but not RICTOR decreased PD-L1 expression, even though RICTOR knockdown decreased phosphorylation of AKT at serine 473 (Fig. 2F).

To determine whether mTOR could regulate other immunosuppressive ligands expressed on tumors, we performed flow cytometry for B7-H4 using the same panel of NSCLC cells

(Supplementary Fig. S1A). Although the majority of these cell lines did not express B7-H4, the highest B7-H4-expressing cell line, H520, was treated with rapamycin. Rapamycin did not alter B7-H4 protein in H520 cells, suggesting that mTOR specifically regulates PD-L1 (Supplementary Fig. S1B). To determine whether other signaling pathways downstream of oncogenic drivers such as the MEK-ERK pathway might play a role in regulating PD-L1, cells were treated with an MEK inhibitor, U0126. U0126 did not alter PD-L1 expression despite inhibiting ERK phosphorylation and proliferation (Supplementary Fig. S2), indicating that control of PD-L1 expression was specific to the PI3K-AKT-mTOR pathway and was not due to stimulation of the MEK-ERK pathway or to indirect effects on cellular proliferation.

Rapamycin decreases PD-L1 expression in murine lung tumors

To validate these *in vitro* studies, we examined the effects of rapamycin on PD-L1 expression *in vivo*. One year after exposure to NNK, 1 week of rapamycin treatment significantly reduced mTOR signaling and decreased PD-L1 expression in A/J mouse lung tumors compared with vehicle-treated lung tumors (Fig. 3A). Similarly, lung tumors from KRAS^{LA2} mice treated for 10 weeks with rapamycin also had lower PD-L1 expression and mTOR activation compared with vehicle-treated littermates (Fig. 3B). Six weeks after doxycycline administration, mutant EGFR^{L858R/T790M} mice were treated for 1 week with vehicle or rapamycin. Lung tumors from mice treated with rapamycin had reduced mTOR activation and PD-L1 expression compared to vehicle-treated mice (Fig. 3C). These studies indicate that mTOR activation is correlated with PD-L1 expression in murine lung tumors.

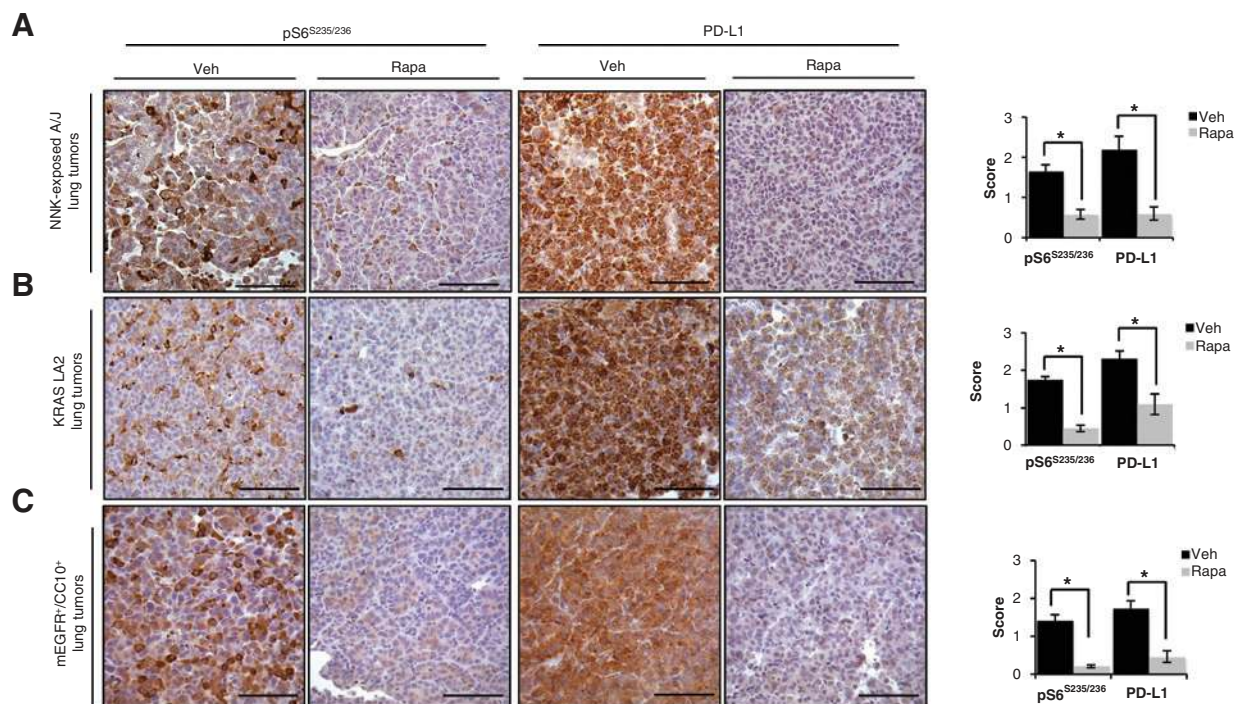


Figure 3. Rapamycin decreases PD-L1 expression in lung tumors *in vivo*. Immunohistochemical staining for pS6 or PD-L1 in lung tumors treated with vehicle or rapamycin from A/J mice exposed to the tobacco-carcinogen NNK (A), C57BL/6 KRAS LA2 mice (B), or dox-exposed FVB mEGFR⁺/CC10⁺ littermates (C). Bar graphs quantify decreased staining of pS6 and PD-L1. Scale bar, 10 μ m. *, $P \leq 0.05$ by unpaired Student *t* test.

Activation of the AKT–mTOR pathway increases PD-L1 expression

On the basis of the observation that inhibition of the PI3K–AKT–mTOR pathway decreases PD-L1 expression, we tested whether cell lines with low basal levels of PD-L1 could increase PD-L1 expression after stimulation of the AKT–mTOR pathway. Administration of EGF to NSCLC cell lines activated the pathway and increased PD-L1 expression (Fig. 4A). Likewise, mouse and human cell lines rapidly activated AKT and mTOR and increased PD-L1 expression (Fig. 4B). Comparison of BEAS-2B cells with BEAS-2B cells fully transformed by NNK showed increased PD-L1 expression and activation of AKT/mTOR in cells fully transformed by NNK (Fig. 4C). Knockdown of PTEN, a negative regulator of PI3K, increased the activation of AKT and PD-L1 expression in CL13 cells (Fig. 4D). To complement the pharmacologic and

genetic results linking active AKT/mTOR signaling to PD-L1 expression in NSCLC, pairs of isogenic HCT116 cells were used to determine whether single genetic alterations of the pathway could increase PD-L1 expression. Increased activation of Akt and mTOR, as well as increased expression of PD-L1 was observed in HCT116 *PTEN*^{-/-} cells, suggesting that regulation of PD-L1 by PTEN may occur in several tumor types. HCT116 cells that express mutant KRAS or mutant PIK3CA alleles also had higher AKT activation and PD-L1 expression compared with isogenic cells with corresponding wild-type alleles (Fig. 4E).

EGF and IFN γ increase PD-L1 protein expression through activation of mTOR

PD-L1 expression can also be induced in tumors in response to proinflammatory cytokines like IFN γ via JAK/STAT signaling and

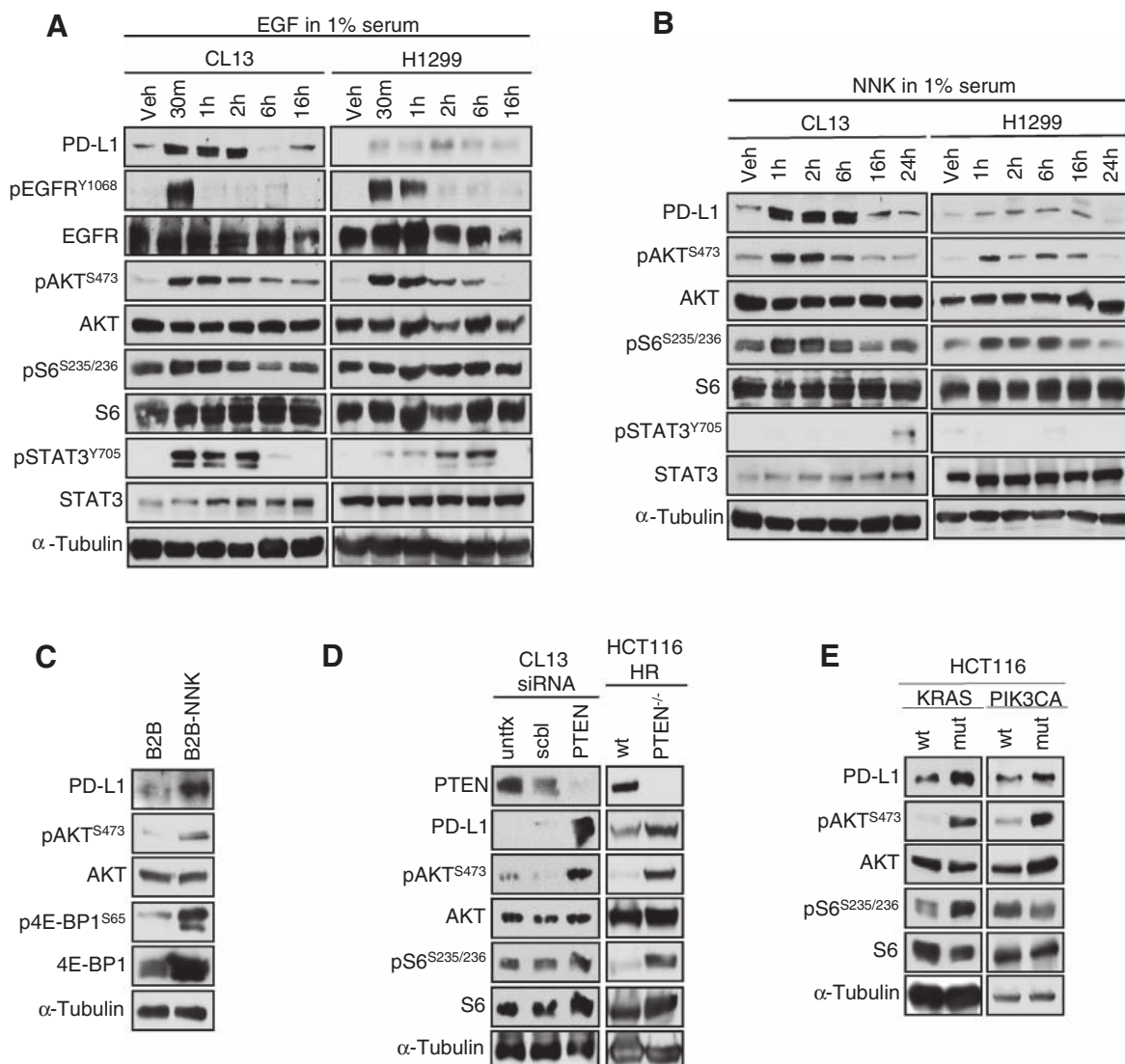


Figure 4.

Activation of the AKT–mTOR pathway increases PD-L1 expression. A, NSCLC cell lines were treated with 5 ng/mL EGF or vehicle in 1% serum. B, NSCLC cell lines were treated with 100 nmol/L NNK or vehicle in 1% serum. C, lysates from B2B and B2B-NNK isogenic cell lines were evaluated by immunoblotting. D, cells were directly transfected with scrambled siRNA or PTEN-targeted siRNA for 24 hours in serum-free media. Cells with wt PTEN or that had lost PTEN are shown on the right. E, comparison of cells that have lost either the mutant KRAS or PIK3CA alleles or the corresponding wt alleles through homologous recombination (HR).

interferon-stimulated response elements in the PD-L1 promoter (7, 28). STAT1 and to a lesser extent STAT3 typically mediates IFN γ signaling. Although both STAT1 and STAT3 can bind to the PD-L1 promoter, STAT3 binds with higher affinity and stimulates more PD-L1 transcript in dendritic cells (DC; ref. 29). Phosphorylation of JAK/STAT occurs minutes after exposure to IFN γ , but in multiple cancer cell lines maximum induction of PD-L1 occurs much later (9–24 hours; ref. 28). For these reasons, we chose to use phospho-STAT3 as a readout for IFN γ signaling and evaluated PD-L1 expression at later time points. Cells were treated with IFN γ for 16 and 24 hours (Fig. 5A). IFN γ activated JAK2 and STAT3 signaling, as well as PD-L1 expression. Parallel cultures of cells were also treated with EGF to compare PD-L1 regulation and signaling pathway activation. Because EGF-stimulated phosphor-

ylation events are rapidly controlled (Fig. 4C), we also included a 30-minute time point to observe EGF-induced AKT and mTOR activation. At 16 hours, EGF and IFN γ increased PD-L1 expression and activated mTOR signaling. Upregulation of PD-L1 was dependent on mTOR activation, because rapamycin pretreatment prevented EGF- and IFN γ -mediated increases in PD-L1 expression, but not IFN γ -induced p-STAT3 (Fig. 5B).

Although EGF and IFN γ induce PD-L1 protein expression in an mTOR-dependent manner, it is unclear whether mTOR exerts transcriptional control of PD-L1. Therefore, we measured PD-L1 transcription. IFN γ increased transcription of *PD-L1* but EGF did not. Rapamycin did not inhibit IFN γ -induced transcription, suggesting that mTOR provides translational control of PD-L1 (Fig. 5C). To confirm translational regulation of PD-L1, NSCLC

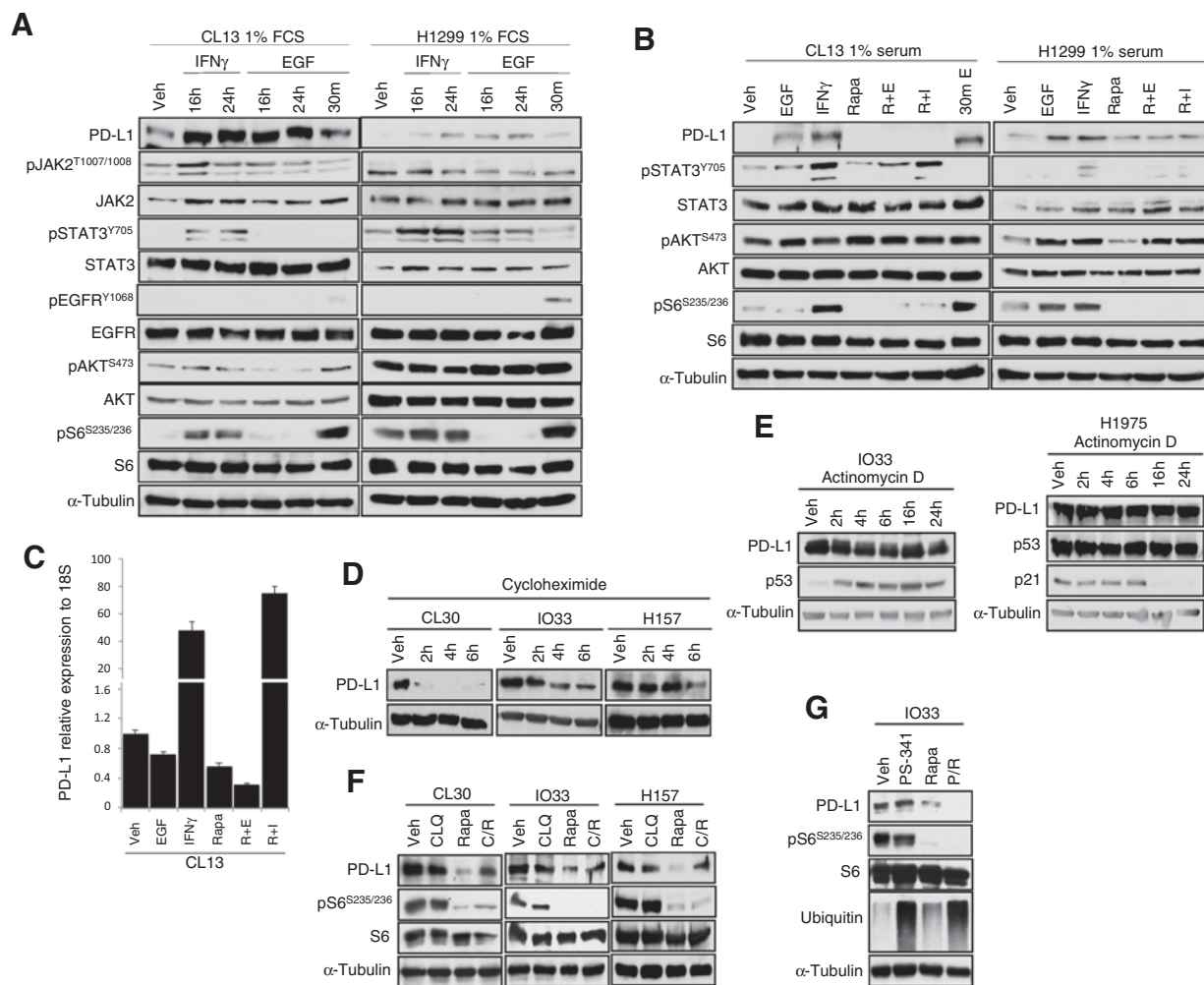


Figure 5.

The AKT-mTOR pathway controls PD-L1 protein expression. A, CL13 and H1299 cell lines were treated with 10 ng/mL IFN γ or 5 ng/mL EGF in 1% serum for the indicated times. An early time point (30 m) was included after EGF addition to confirm pathway activation. B, cells were treated for 24 hours with 100 nmol/L rapamycin alone, for 23 hours with 5 ng/mL EGF or 10 ng/mL IFN γ alone, or the combination by treating with rapamycin for 1 hour, then adding EGF or IFN γ to culture media and harvesting 23 hours later. C, CL13 cells treated as in B and RNA was harvested for RT-PCR. D, cells were treated with 100 μ g/mL cycloheximide for the indicated time points. E, cells were treated with 5 μ g/mL actinomycin D for the indicated time points. Immunoblots shown are representative of three independent experiments. F, cells were treated for 6 hours with 300 μ mol/L chloroquine (CLQ) alone, for 4 hours with 100 nmol/L rapamycin alone, or the combination by treating with CLQ for 2 hours, then adding rapamycin to culture media and harvesting 4 hours later. G, cells were treated for 6 hours with 100 nmol/L PS-341 alone, for 5 hours with 100 nmol/L rapamycin alone, or the combination by treating with PS-341 for 2 hours, then adding rapamycin to culture media and harvesting 5 hours later.

Table 1. mTOR activation is required, but may not be sufficient to induce PD-L1 expression in primary lung adenocarcinoma and squamous cell carcinoma

		Membrane PD-L1		P	95% CI	
		Cases	Negative			Positive
pS6 ^{S235/236}	Negative	42	35	7	<0.001	2.33–17.0
	Positive	116	53	63		

NOTE: Correlation between p-S6^{S235/236} and PD-L1 markers in the TMAs. Statistical analyses were performed using the Fisher exact test.

cell lines were exposed to the protein translation inhibitor cycloheximide (Fig. 5D). Cycloheximide rapidly decreased PD-L1 protein expression, indicating that PD-L1 likely has rapid turnover in lung cancer cells. In contrast with cycloheximide, inhibiting transcription with actinomycin D did not change PD-L1 expression, even at later time points (Fig. 5E). The accumulation of p53 in IO33 cells and the accumulation of p21 in the mutant p53 cell line H1975 demonstrated that transcription was successfully inhibited. These results suggest that PD-L1 expression is predominantly controlled at the protein level and that mTOR exerts its regulation at this level.

To examine how rapamycin was decreasing PD-L1 protein expression, we studied two main pathways of protein degradation via the lysosome or the proteasome. Pretreatment with a lysosome acidification inhibitor (chloroquine) but not a proteasome inhibitor (PS-341) prevented rapamycin-mediated decreases in PD-L1 protein (Fig. 5F and G). This suggests that rapamycin inhibits PD-L1 expression through a combination of decreased protein synthesis and increased lysosomal protein degradation.

Expression of PD-L1 and activation of mTOR in human lung adenocarcinomas and squamous cell carcinomas

To determine whether these findings are clinically relevant, two human lung tissue microarrays (TMA) were stained and scored for membranous and/or cytoplasmic PD-L1 expression (Supplementary Fig. S3). One TMA included 63 lung adenocarcinomas with matched normal lung and assorted normal tissues. The other TMA contained 96 lung squamous cell carcinomas with assorted normal tissues. These normal tissues served as internal positive (placenta) or negative (soft tissue) controls for PD-L1 expression. Each TMA was simultaneously stained with an IgG antibody to control for background. Clinical and pathologic characteristics of the patient population are summarized in Supplementary Table S1. Sixty-two of 63 adenocarcinoma and 96 of 96 squamous cell carcinoma tumors were evaluable. Twenty of 62 (32.2%) lung adenocarcinomas and 50 of 96 (52.1%) lung squamous cell carcinomas expressed membranous PD-L1, which is consistent with previous observations (Supplementary Fig. S3B and S3D; refs. 30–34). No clinical or pathologic characteristics were associated with PD-L1 expression. PD-L1 membranous expression was observed on lung tumor tissue and on resident alveolar macrophages, but not on non-neoplastic lung tissue. These data support a potential common role of this protein in mediating immunosuppression in NSCLC.

To explore the potential regulation of PD-L1 in human primary lung tumors by mTOR activation, both TMAs were also stained with an antibody specific for phosphorylation of S6 at S235/236 (Supplementary Fig. S3C and S3D). Because there were no significant differences between the TMA characteristics (Supplementary Table S1; stage significance is likely due to a sample size bias), the adenocarcinomas and squamous cell carcinomas were

combined for further analyses. Approximately 90% of tumors with PD-L1 expression had activation of mTOR and 54% of tumors with mTOR activation also expressed PD-L1, suggesting that mTOR activation was necessary, but not sufficient, for PD-L1 expression (Table 1). Distribution of mTOR activation tended to be similar to staining patterns for PD-L1, suggesting that the same cells co-express both markers (Supplementary Fig. S4). The majority (83%) of tumors negative for pS6 were also negative for PD-L1. A small subset of tumors expressed PD-L1 without mTOR activation, indicating that there may be additional mechanisms inducing PD-L1 expression. Sixty-three of 158 (40%) of lung tumors had both active mTOR signaling and PD-L1 expression, and a Fisher exact test revealed a statistically significant correlation between the two markers ($P = 0.0001$; Table 1). These results underscore the clinical relevance of our preclinical associations.

The combination of rapamycin and a PD-1 blocking antibody decreases lung tumor growth

Monoclonal antibodies that block PD-L1 or PD-1 have shown clinical benefit in NSCLC (9, 10). However, it is possible that simultaneous inhibition of both PD-L1 and PD-1 may increase therapeutic benefit because each has additional immunosuppressive binding partners. To test the efficacy of systemically blocking PD-1 while reducing the expression of PD-L1 in tumor tissue, a murine anti-PD-1 antibody and rapamycin were administered in the KRAS^{LA2} mouse model (Fig. 6A). Rapamycin alone decreased the tumor burden of KRAS-driven lung tumors by approximately 50% whereas PD-1 blockade had no effect as a single agent (Fig. 6B). The combination of rapamycin and anti-PD-1 significantly reduced lung tumor burden by comparison with any other treatment group. The combination therapy increased CD3⁺ T cells and reduced FoxP3⁺ Tregs (Fig. 6C). This led to a higher ratio of CD3⁺ T cells to Tregs, indicating a shift towards an immune activated rather than immunosuppressive microenvironment. Lung tumors from mice treated with rapamycin had a reduction in PD-L1 expression and mTOR activation (Fig. 6D and E). A marker of apoptosis, cleaved caspase-3, was increased in tumors treated with the combination. Although rapamycin alone inhibited tumor proliferation, tumors treated with the combination also had more pHP1 γ ⁺ cells, suggesting that these tumors had undergone senescence. These findings demonstrate enhanced antitumor efficacy with the combination of rapamycin and a PD-1 blocking antibody through increased apoptosis and cellular senescence. We confirmed the efficacy of rapamycin and PD-1 blockade in a second mouse model of KRAS-driven lung cancer (Supplementary Figs. S5 and S6). These findings demonstrate enhanced antitumor efficacy against two mutant KRAS mouse models of lung cancer when rapamycin and a PD-1 blocking antibody are combined.

Discussion

PD-L1 plays a prominent role in the balance of the immune system between the stimulatory signals needed for effective immune responses and maintenance of self-tolerance or tissue integrity. PD-L1 can be expressed on hematopoietic and non-hematopoietic cells, as well as in lymphoid and peripheral tissues. Consequently, the regulation of PD-L1 is complex and most likely depends on the status of underlying transcriptional and signaling networks. Here, our studies reveal a strong association between PD-L1 protein and activation of the AKT–mTOR pathway in lung cancer. The dependence of PD-L1 expression on mTOR is

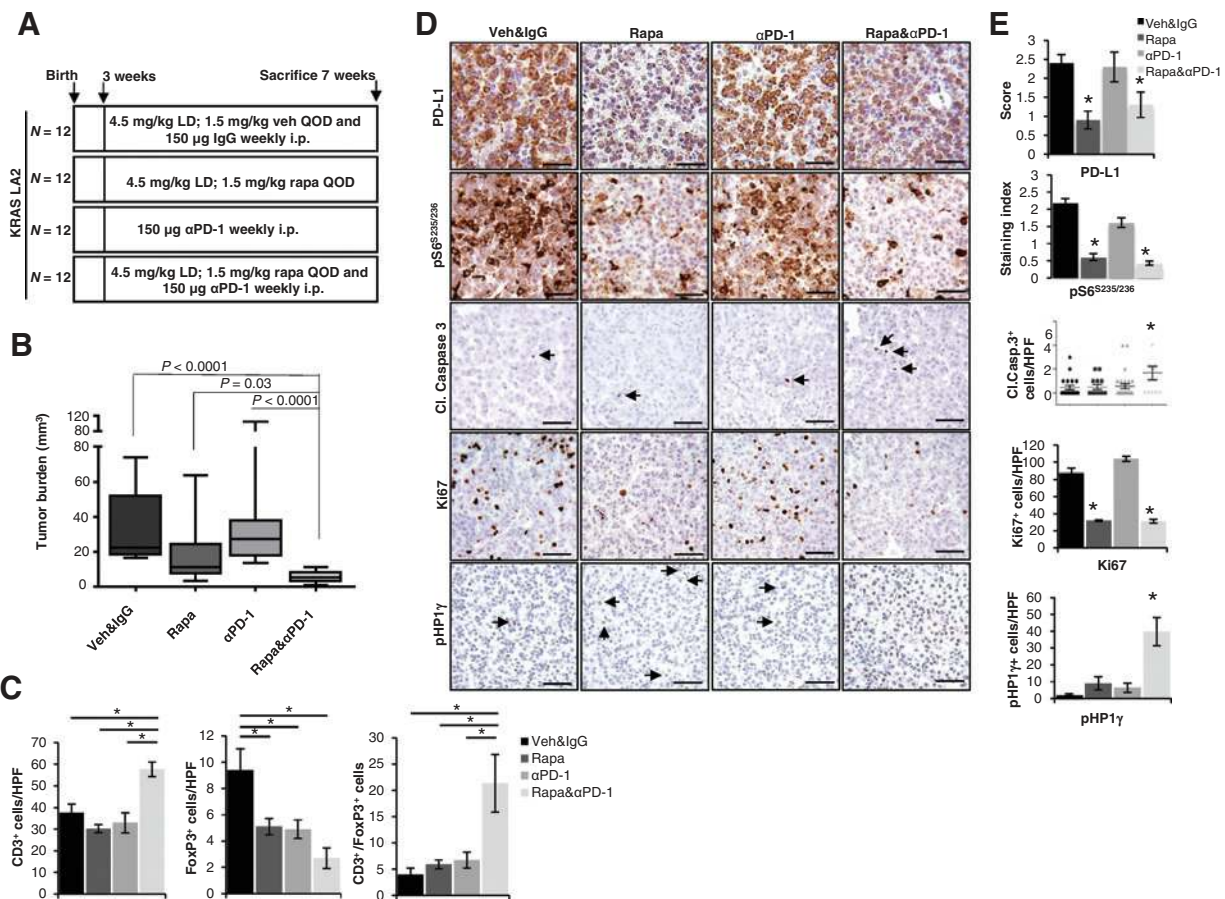


Figure 6.

The combination of rapamycin and α PD-1 blockade significantly reduces lung tumor burden in the KRAS LA2 mouse model. A, KRAS LA2 mice were treated with either IP vehicle and IgG, rapamycin, α PD-1 antibody, or rapamycin and α PD-1 for 4 weeks beginning at the time of weaning. B, tumor burden after 4 weeks of treatment; *, $P \leq 0.05$ by Mann-Whitney. C, quantification of IHC staining for CD3⁺ or FoxP3⁺ cells. The ratio of CD3⁺ over FoxP3⁺ cells is also shown; *, $P \leq 0.05$ by two-way ANOVA. D, images represent IHC staining for PD-L1, pS6, cleaved caspase-3, Ki67, and pHP1 γ . Scale bar, 10 μ m. E, quantification of IHC stains in D. *, $P \leq 0.05$ by two-way ANOVA.

consistent with studies in glioma, breast, prostate, ovarian, and pancreatic cancer. Interestingly, this relationship does not extend to melanoma, emphasizing multiple mechanisms for PD-L1 regulation in solid tumors (35).

Our TMA study suggested that mTOR activation is necessary but not sufficient for PD-L1 expression. It is possible that tumors with mTOR activation but no PD-L1 protein lack *PD-L1* transcripts, which would preclude mTOR-dependent translation. Approximately 53% (810/1,537) of lung cancer specimens in The Cancer Genome Atlas set do not have detectable *PD-L1* mRNA (36). Other studies have identified that *PD-L1* mRNA levels were only higher than normal lung tissue in stage IV lung tumors (37). Thus, there may be additional levels of PD-L1 regulation between transcription and translation. A recent study directly compared samples for *PD-L1* mRNA and protein expression and observed that *PD-L1* mRNA had a complex, nonlinear positive association with PD-L1 protein expression. This finding was consistent in two separate TMA cohorts and suggests that PD-L1 is regulated at both transcription and translational levels (34). In DCs, LPS and IFN γ -mediated induction of PD-L1 protein depends on both active transcription and translation (38). The relative contribution of

regulatory steps on PD-L1 expression will probably depend on cell type, context, and may vary over the course of response to a stimulus.

Transcription of PD-L1 can be induced by many cytokines, of which IFN γ is the most potent (7). Activation of the AKT-mTOR pathway plays a central role in the initiation of IFN-stimulated gene translation, in a mechanism parallel to but independent of activation of the JAK-STAT pathway (39). Therefore, although *PD-L1* transcription does not depend on mTOR activation, translation of IFN γ -induced transcripts, including *PD-L1*, may be dependent on activation of PI3K, AKT, and mTOR kinase activity. The dependence of PD-L1 translation on PI3K-AKT-mTOR activity is also observed during viral infections. In HIV-1-infected macrophages and dendritic cells, the viral protein Nef induces *PD-L1* transcription by binding to the promoter but PD-L1 protein expression depends on active PI3K/AKT signaling (40). Our data indicate that multiple types of stimuli, including growth factors cytokines and oncogenes, converge at mTOR to increase PD-L1 expression.

Inhibiting ligation of tumor-derived PD-L1 with PD-1 on T cells is proposed as a major therapeutic target to revert tumor-mediated

immunosuppression. However, because PD-L1 and PD-1 have additional binding partners perhaps blocking multiple interactions is needed to fully rescue antitumor immunity. Combining PD-1 blockade with rapamycin, which inhibited oncogenic KRAS signaling and PD-L1 expression, resulted in a significant reduction in tumor burden compared with either drug alone. Only the combination therapy significantly increased the ratio of CD3⁺ to FoxP3⁺ cells, supporting this change in T-cell populations as a readout for antitumor activity. In addition, only the combination was associated with decreased proliferation and increased apoptotic and senescent markers. Drug-induced senescence with DNA-damaging agents is well established, but a role for adaptive immunity in driving cancer cell senescence was recently identified. In multiple murine models and in human cancers, T helper 1 cell production of IFN γ and TNF α induce immune-dependent tumor cell senescence (41). Although this is the first demonstration of immune-induced senescence in tumors, immune cells promote senescence to regulate other leukocytes. For example, Tregs can induce senescence in naïve and memory T cells through a mechanism dependent on toll like receptor 8, p38, and ERK1/2 (42). A remarkable aspect of checkpoint blockade with PD-1 or PD-L1 is the generation of long-term stable disease in the absence of complete tumor regression, raising the possibility that these tumors have undergone senescence.

Implementing rapamycin as a cancer therapy raises issues about its own role in immunosuppression. Rapamycin has a black box warning from the FDA stemming from a study of renal transplant patients who were also taking cyclosporine and corticosteroids (43), but multiple trials of single-agent rapamycin or rapamycin analogues in cancer patients have shown no evidence of increased incidence of immunosuppression (25, 44). In fact, many basic and clinical studies have associated rapamycin with active immune responses (45, 46). Our studies in the NNK-induced lung cancer model have shown only modest decreases in CD4⁺ levels with short-term or continuous rapamycin treatment. Factors that are likely to play important roles in the cumulative effects of rapamycin on the immune system include the timing and degree of mTOR inhibition, as well as cell type and modulation of mTORC2 signaling. Although precise mechanisms remain unclear, we demonstrate the potential to use rapamycin in combination with a PD-1 blocking antibody to increase antitumor immunity. Rapamycin administration has been shown to sensitize tumors to immunotherapy in other mouse model systems. For example, treatment of fibrosarcoma or colorectal cancers with rapamycin increased tumor sensitivity to adoptive cellular immunotherapy (47). Although PD-L1 expression was not examined in this study, it is tempting to speculate PD-L1 as a contributing factor in immunosuppression.

Responses to PD-1 and PD-L1 blockade have been proposed to be associated with the presence of PD-L1 and many ongoing clinical trials require PD-L1⁺ pretreatment biopsies. Despite strong expression of PD-L1 in lung tumors, PD-1 blockade had no effect on tumorigenesis in the KRAS^{LA2} mouse model. This is in agreement with a report demonstrating PD-1 blockade reduced tumor burden in mouse models of mutant EGFR- but not KRAS-driven lung cancer (16). Because both mutant EGFR and KRAS tumor models express PD-L1, this may indicate specific genomic subsets of lung tumors predict response to single-agent anti-PD-1 outside of PD-L1 expression. However, multiple clinical studies have not identified the presence of mutant KRAS or EGFR as predictors for successful PD-1 blockade (48, 49). In addition to

PD-L1 expression, it is possible that response to PD-1 or PD-L1 blockade depends on a critical threshold of TILs at the start of therapy (50). We have observed that the number of tumor-infiltrating CD3⁺ T cells per high powered field is doubled in the mutant EGFR^{L858R/T790M} compared with the KRAS^{LA2} mouse model (88.9 vs. 37.5 CD3⁺ T cells; unpublished data). Furthermore, a recent study demonstrated higher nonsynonymous mutational burden is associated with response to PD-1 blockade as a single agent, in part by enhancing neoantigen-specific CD8⁺ T-cell responses (51). Identifying the mechanisms responsible for the differences in lung tumors and TILs between responders and non-responders of PD-1 blockade would have important insight into therapeutic biomarkers.

Activation of PI3K-AKT-mTOR signaling is driven by multiple mechanisms in NSCLC and is vital to tumor development, progression, and prognosis. We show that activation of AKT-mTOR, regardless of the driving oncogene or exogenous stimulus, increases PD-L1 protein expression in NSCLC. Our data extend a growing body of evidence that oncogenes have tumor cell autonomous effects by altering the immune system in the tumor microenvironment. Clinical trials combining anti-PD-1 antibodies and current standard-of-care treatments are already underway and include combining targeted therapies with immunotherapy (73–75). Our studies provide rationale to combine and optimize PI3K-AKT-mTOR inhibitors with anti-PD-1 antibodies.

Disclosure of Potential Conflicts of Interest

J.M. Taube reports receiving a commercial research grant and is a consultant/advisory board member for Bristol Myers Squibb. No potential conflicts of interest were disclosed by the other authors.

Authors' Contributions

Conception and design: K.J. Lastwika, W. Wilson III, S. Yao, L.N. Liu, P.A. Dennis

Development of methodology: W. Wilson III, J. Norris, H. Xu, P.A. Dennis

Acquisition of data (provided animals, acquired and managed patients, provided facilities, etc.): K.J. Lastwika, J. Norris, H. Kitagawa, S. Kawabata, P.A. Dennis

Analysis and interpretation of data (e.g., statistical analysis, biostatistics, computational analysis): K.J. Lastwika, S.R. Ghazarian, S. Kawabata, J.M. Taube, P.A. Dennis

Writing, review, and/or revision of the manuscript: K.J. Lastwika, W. Wilson III, Q.K. Li, S.R. Ghazarian, H. Kitagawa, J.M. Taube, S. Yao, J.J. Gills, P.A. Dennis

Administrative, technical, or material support (i.e., reporting or organizing data, constructing databases): Q.K. Li, S. Kawabata, S. Yao, P.A. Dennis

Study supervision: P.A. Dennis

Acknowledgments

The authors thank Dr. Leiping Chen for providing the anti-PD-L1 monoclonal antibody 5H1.

Grant Support

This work was supported by intramural funding from the National Cancer Institute, the George Washington University, and NIH grant P30 CA006973.

The costs of publication of this article were defrayed in part by the payment of page charges. This article must therefore be hereby marked *advertisement* in accordance with 18 U.S.C. Section 1734 solely to indicate this fact.

Received November 19, 2014; revised August 30, 2015; accepted September 20, 2015; published OnlineFirst December 4, 2015.

References

- Siegel R, Ma J, Zou Z, Jemal A. Cancer statistics, 2014. *CA Cancer J Clin* 2014;64:9–29.
- Memmott RM, Mercado JR, Maier CR, Kawabata S, Fox SD, Dennis PA. Metformin prevents tobacco carcinogen-induced lung tumorigenesis. *Cancer Prev Res* 2010;3:1066–76.
- Granville CA, Warfel N, Tsurutani J, Hollander MC, Robertson M, Fox SD, et al. Identification of a highly effective rapamycin schedule that markedly reduces the size, multiplicity, and phenotypic progression of tobacco carcinogen-induced murine lung tumors. *Clin Cancer Res* 2007;13:2281–9.
- Hollander MC, Maier CR, Hobbs EA, Ashmore AR, Linnoila RI, Dennis PA. Akt1 deletion prevents lung tumorigenesis by mutant K-ras. *Oncogene* 2011;30:1812–21.
- Granville CA, Memmott RM, Balogh A, Mariotti J, Kawabata S, Han W, et al. A central role for Foxp3⁺ regulatory T cells in K-Ras-driven lung tumorigenesis. *PLoS ONE* 2009;4:e5061.
- Dong H, Zhu G, Tamada K, Chen L. B7-H1, a third member of the B7 family, co-stimulates T-cell proliferation and interleukin-10 secretion. *Nat Med* 1999;5:1365–9.
- Dong H, Strome SE, Salomao DR, Tamura H, Hirano F, Flies DB, et al. Tumor-associated B7-H1 promotes T-cell apoptosis: a potential mechanism of immune evasion. *Nat Med* 2002;8:793–800.
- Butte MJ, Keir ME, Phamduy TB, Sharpe AH, Freeman GJ. Programmed death-1 ligand 1 interacts specifically with the B7-1 costimulatory molecule to inhibit T-cell responses. *Immunity* 2007;27:111–22.
- Topalian SL, Hodi FS, Brahmer JR, Gettinger SN, Smith DC, McDermott DF, et al. Safety, activity, and immune correlates of anti-PD-1 antibody in cancer. *N Engl J Med* 2012;366:2443–54.
- Brahmer JR, Tykodi SS, Chow LQM, Hwu WJ, Topalian SL, Hwu P, et al. Safety and activity of anti-PD-L1 antibody in patients with advanced cancer. *N Engl J Med* 2012;366:2455–65.
- Lipson EJ, Sharfman WH, Drake CG, Wollner I, Taube JM, Anders RA, et al. Durable cancer regression off-treatment and effective reinduction therapy with an anti-PD-1 antibody. *Clin Cancer Res* 2013;19:462–8.
- Green MR, Monti S, Rodig SJ, Juszczynski P, Currie T, O'Donnell E, et al. Integrative analysis reveals selective 9p24.1 amplification, increased PD-1 ligand expression, and further induction via JAK2 in nodular sclerosing Hodgkin lymphoma and primary mediastinal large B-cell lymphoma. *Blood* 2010;116:3268–77.
- Marzec M, Zhang Q, Goradia A, Raghunath PN, Liu X, Paessler M, et al. Oncogenic kinase NPM/ALK induces through STAT3 expression of immunosuppressive protein CD274 (PD-L1, B7-H1). *Proc Natl Acad Sci U S A* 2008;105:20852–7.
- Parsa AT, Waldron JS, Panner A, Crane CA, Parney IF, Barry JJ, et al. Loss of tumor suppressor PTEN function increases B7-H1 expression and immunoresistance in glioma. *Nat Med* 2007;13:84–8.
- Crane CA, Panner A, Murray JC, Wilson SP, Xu H, Chen L, et al. PI(3) kinase is associated with a mechanism of immunoresistance in breast and prostate cancer. *Oncogene* 2009;28:306–12.
- Akbay EA, Koyama S, Carretero J, Altobelli A, Tchaicha JH, Christensen CL, et al. Activation of the PD-1 pathway contributes to immune escape in EGFR-driven lung tumors. *Cancer Discov* 2013;3:1355–63.
- Xu C, Fillmore CM, Koyama S, Wu H, Zhao Y, Chen Z, et al. Loss of Lkb1 and Pten leads to lung squamous cell carcinoma with elevated PD-L1 expression. *Cancer Cell* 2014;25:590–604.
- D'Incecco A, Andreozzi M, Ludovini V, Rossi E, Capodanno A, Landi L, et al. PD-1 and PD-L1 expression in molecularly selected non-small cell lung cancer patients. *Br J Cancer* 2015;112:95–102.
- Garon EB, Rizvi NA, Hui R, Leigh N, Balmanoukian AS, Eder JP, et al. Pembrolizumab for the treatment of non-small cell lung cancer. *N Engl J Med* 2015;372:2018–28.
- Jones-Bolin SE, Johansson E, Palmisano WA, Anderson MW, Wiest JS, Belinsky SA. Effect of promoter and intron 2 polymorphisms on murine lung K-ras gene expression. *Carcinogenesis* 1998;19:1503–8.
- Klein-Szanto AJ, Iizasa T, Momiki S, Garcia-Palazzo I, Caamano J, Metcalf R, et al. A tobacco-specific N-nitrosamine or cigarette smoke condensate causes neoplastic transformation of xenotransplanted human bronchial epithelial cells. *Proc Natl Acad Sci U S A* 1992;89:6693–7.
- Sarbassov DD, Guertin DA, Ali SM, Sabatini DM. Phosphorylation and regulation of Akt/PKB by the rictor–mTOR complex. *Science* 2005;307:1098–101.
- Politi K, Zakowski MF, Fan PD, Schonfeld EA, Pao W, Varmus HE. Lung adenocarcinomas induced in mice by mutant EGF receptors found in human lung cancers respond to a tyrosine kinase inhibitor or to down-regulation of the receptors. *Genes Dev* 2006;20:1496–510.
- Johnson L, Mercer K, Greenbaum D, Bronson RT, Crowley D, Tuveson DA, et al. Somatic activation of the K-ras oncogene causes early onset lung cancer in mice. *Nature* 2001;410:1111–6.
- O'Donnell A, Faivre S, Burris HA III, Rea D, Papadimitrakopoulou V, Shand N, et al. Phase I pharmacokinetic and pharmacodynamic study of the oral mammalian target of rapamycin inhibitor everolimus in patients with advanced solid tumors. *J Clin Oncol* 2008;26:1588–95.
- Taube JM, Anders RA, Young GD, Xu H, Sharma R, McMiller TL, et al. Colocalization of inflammatory response with B7-h1 expression in human melanocytic lesions supports an adaptive resistance mechanism of immune escape. *Sci Transl Med* 2012;4:127ra37.
- West KA, Linnoila IR, Belinsky SA, Harris CC, Dennis PA. Tobacco carcinogen-induced cellular transformation increases activation of the phosphatidylinositol 3'-kinase/Akt pathway *in vitro* and *in vivo*. *Cancer Res* 2004;64:446–51.
- Lee SJ, Jang BC, Lee SW, Yang YI, Suh SI, Park YM, et al. Interferon regulatory factor-1 is prerequisite to the constitutive expression and IFN-gamma-induced upregulation of B7-H1 (CD274). *FEBS Lett* 2006;580:755–62.
- Wolfe SJ, Strebosky J, Bartz H, Sahr A, Arnold C, Kaiser C, et al. PD-L1 expression on tolerogenic APCs is controlled by STAT-3. *Eur J Immunol* 2011;41:413–24.
- Mu CY, Huang JA, Chen Y, Chen C, Zhang XG. High expression of PD-L1 in lung cancer may contribute to poor prognosis and tumor cells immune escape through suppressing tumor infiltrating dendritic cells maturation. *Med Oncol* 2011;28:682–8.
- Chen YB, Mu CY, Huang JA. Clinical significance of programmed death-1 ligand-1 expression in patients with non-small cell lung cancer: a 5-year follow-up study. *Tumori* 2012;98:751–5.
- Boland JM, Kwon ED, Harrington SM, Wampfler JA, Tang H, Yang P, et al. Tumor B7-H1 and B7-H3 expression in squamous cell carcinoma of the lung. *Clin Lung Cancer* 2013;14:157–63.
- Konishi J, Yamazaki K, Azuma M, Kinoshita I, Dosaka-Akita H, Nishimura M. B7-H1 expression on non-small cell lung cancer cells and its relationship with tumor-infiltrating lymphocytes and their PD-1 expression. *Clin Cancer Res* 2004;10:5094–100.
- Velcheti V, Schalper KA, Carvajal DE, Anagnostou VK, Syrigos KN, Sznol M, et al. Programmed death ligand-1 expression in non-small cell lung cancer. *Lab Invest* 2014;94:107–16.
- Jiang X, Zhou J, Giobbie-Hurder A, Wargo J, Hodi FS. The activation of MAPK in melanoma cells resistant to BRAF inhibition promotes PD-L1 expression that is reversible by MEK and PI3K inhibition. *Clin Cancer Res* 2013;19:598–609.
- Rhodes DR, Kalyana-Sundaram S, Mahavisno V, Varambally R, Yu J, Briggs BB, et al. OncoPrint 3.0: genes, pathways, and networks in a collection of 18,000 cancer gene expression profiles. *Neoplasia* 2007;9:166–80.
- Sasaki H, Suzuki A, Shitara M, Hikosaka Y, Okuda K, Moriyama S, et al. gene expression in Japanese lung cancer patients. *Biomed Rep* 2013;1:93–6.
- Loke P, Allison JP. PD-L1 and PD-L2 are differentially regulated by Th1 and Th2 cells. *Proc Natl Acad Sci U S A* 2003;100:5336–41.
- Kaur S, Sassano A, Dolniak B, Joshi S, Majchrzak-Kita B, Baker DP, et al. Role of the Akt pathway in mRNA translation of interferon-stimulated genes. *Proc Natl Acad Sci U S A* 2008;105:4808–13.
- Muthumani K, Shedlock DJ, Choo DK, Fagone P, Kawalekar OU, Goodman J, et al. HIV-mediated phosphatidylinositol 3-kinase/serine-threonine kinase activation in APCs leads to programmed death-1 ligand upregulation and suppression of HIV-specific CD8 T cells. *J Immunol* 2011;187:2932–43.
- Braumuller H, Wieder T, Brenner E, Assmann S, Hahn M, Alkhaled M, et al. T-helper-1-cell cytokines drive cancer into senescence. *Nature* 2013;494:361–5.

42. Ye J, Huang X, Hsueh EC, Zhang Q, Ma C, Zhang Y, et al. Human regulatory T cells induce T-lymphocyte senescence. *Blood* 2012;120:2021–31.
43. Hidalgo M, Buckner JC, Erlichman C, Pollack MS, Boni JP, Dukart G, et al. A phase I and pharmacokinetic study of temsirolimus (CCI-779) administered intravenously daily for 5 days every 2 weeks to patients with advanced cancer. *Clin Cancer Res* 2006;12:5755–63.
44. Bissler JJ, McCormack FX, Young LR, Elwing JM, Chuck G, Leonard JM, et al. Sirolimus for angiomyolipoma in tuberous sclerosis complex or lymphangioleiomyomatosis. *N Engl J Med* 2008;358:140–51.
45. Haydar AA, Denton M, West A, Rees J, Goldsmith DJ. Sirolimus-induced pneumonitis: three cases and a review of the literature. *Am J Transplant* 2004;4:137–9.
46. Rao RR, Li Q, Odunsi K, Shrikant PA. The mTOR kinase determines effector versus memory CD8⁺ T-cell fate by regulating the expression of transcription factors T-bet and Eomesodermin. *Immunity* 2010;32:67–78.
47. Hahnel PS, Thaler S, Antunes E, Huber C, Theobald M, Schuler M. Targeting AKT signaling sensitizes cancer to cellular immunotherapy. *Cancer Res* 2008;68:3899–906.
48. Garon EB, Balmanoukian A, Hamid O, Hui R, Gandhi L, Leighl N, et al. Abstract A20: MK-3475 monotherapy for previously treated non-small cell lung cancer (NSCLC): preliminary safety and clinical activity. *Clin Cancer Res* 2014;20(2 Suppl):A20-A.
49. Creelan BC. Update on immune checkpoint inhibitors in lung cancer. *Cancer Control* 2014;21:80–9.
50. Herbst RS, Soria JC, Kowanetz M, Fine GD, Hamid O, Gordon MS, et al. Predictive correlates of response to the anti-PD-L1 antibody MPDL3280A in cancer patients. *Nature* 2014;515:563–7.
51. Rizvi NA, Hellmann MD, Snyder A, Kvistborg P, Makarov V, Havel JJ, et al. Cancer immunology. Mutational landscape determines sensitivity to PD-1 blockade in non-small cell lung cancer. *Science* 2015;348:124–8.